Expression of varicella-zoster virus VLT-ORF63 fusion transcript induces broad viral gene expression during reactivation from neuronal latency

Werner J. D. Ouwendijk[1, 7], Daniel P. Depledge[2, 7], Labchan Rajbhandari[3], Tihana Lenac Rovis[4], Stipan Jonjic[4], Judith Breuer[5], Arun Venkatesan[3], Georges M. G. M. Verjans[1], and Tomohiko Sadaoka[6*]

Author Affiliation:

[1]Department of Viroscience, Erasmus Medical Centre, 3015 CN, Rotterdam, The Netherlands.

[2]Department of Medicine, New York University School of Medicine, NY 10016, United States of America.

[3]Division of Neuroimmunology and Neuroinfectious Diseases, Department of Neurology, Johns Hopkins University School of Medicine, 600 N. Wolfe St., Meyer 6-113, Baltimore, Maryland 21287, United States of America.

[4]Centre for Proteomics, Faculty of Medicine, University of Rijeka, Rijeka 51000, Croatia

[5]Division of Infection and Immunity, University College London, London, WC1E 6BT, United Kingdom.

[6]Division of Clinical Virology, Center for Infectious Diseases, Kobe University Graduate School of Medicine, 7-5-1 Kusunoki-cho, Chuo-ku, Kobe, 650-0017, Japan.

[7]These authors contributed equally: Werner J. D. Ouwendijk and Daniel P. Depledge.

***Corresponding Author:**

Tomohiko Sadaoka, DDS, PhD

Assistant Professor, Division of Clinical Virology, Center for Infectious Diseases

Kobe University Graduate School of Medicine, 7-5-1 Kusunoki-cho, Chuo-ku, Kobe, 650-0017, Japan.

Email: tomsada@crystal.kobe-u.ac.jp

ORCID identifier:

Werner J. D. Ouwendijk, https://orcid.org/0000-0001-8393-296X

Daniel P. Depledge, https://orcid.org/0000-0002-4292-0599

Labchan Rajbhandari, https://orcid.org/0000-0002-9252-2580

Tihana Lenac Rovis, https://orcid.org/0000-0002-3299-1334

Stipan Jonjic, https://orcid.org/0000-0001-5003-3108

Judith Breuer, https://orcid.org/0000-0001-8246-0534

Arun Venkatesan, https://orcid.org/0000-0002-9335-7361

Georges M. G. M. Verjans, https://orcid.org/0000-0002-2465-2674

Tomohiko Sadaoka, http://orcid.org/0000-0001-7951-6904

Author Contributions:

W.J.D.O., D.P.D., and T.S. designed the study, performed the experiments and analyzed the data. W.J.D.O., D.P.D., G.M.G.M.V., and T.S. wrote the paper. L.R., T.L.R., S.J., and A.V.

contributed to new reagents/analytic tools. J.B. and G.M.G.M.V. provided additional input into the study. All authors read and approved the final paper.

Summary

Varicella-zoster virus (VZV) establishes lifelong neuronal latency in most humans world-wide, reactivating in one-third to cause herpes zoster and occasionally chronic pain. How VZV establishes, maintains and reactivates from latency is largely unknown. Latent VZV gene expression is restricted to VZV latency-associated transcript (VLT) and open reading frame 63 (ORF63) in naturally VZV-infected human trigeminal ganglia (TG). Notably, these transcript levels positively correlated suggesting co-regulated transcription during latency. Here, we used direct RNA-sequencing to identify fusion transcripts that combine VLT and ORF63 loci (VLT-ORF63) and are expressed during both lytic and latent VZV infections. Furthermore, real-time PCR, RNA *in situ* hybridization and 5' rapid amplification of cDNA ends (RACE) all confirmed VLT-ORF63, but not canonical ORF63, expression in human TG. During lytic infection, one of the two major VLT-ORF63 isoforms encodes a novel fusion protein combining VLT and ORF63 proteins (pVLT-ORF63). *In vitro*, VLT is transcribed in latently VZV-infected human sensory neurons, whereas VLT-ORF63 expression is induced by reactivation stimuli. Moreover, the pVLT-ORF63-encoding VLT-ORF63 isoform induced transcription of lytic VZV genes. Collectively, our findings show that VZV expresses a unique set of VLT-ORF63 transcripts, potentially involved in the transition from latency to lytic VZV infection.

66 **Main Text**

67

68 The ubiquitous human neurotropic alphaherpesvirus (αHV) varicella-zoster virus (VZV)
69 establishes lifelong latency in sensory neurons of dorsal root and cranial nerve ganglia,
70 as well as autonomic and enteric ganglia[1,2]. VZV reactivates in about one-third of latently
71 infected individuals to cause herpes zoster (HZ), a debilitating disease often complicated
72 by post-herpetic neuralgia (PHN)[3,4]. The incidence and severity of HZ is closely related to
73 declining VZV-specific T-cell immunity by natural senescence[5], and immunosuppressive
74 diseases[6]. However, the mechanisms governing how VZV reestablishes a lytic infection
75 from latency in neurons, especially the identity of the viral gene(s) that facilitate
76 reactivation in response to cellular signaling, remain unknown.

77 During latency in human trigeminal ganglia (TG), VZV gene expression is restricted
78 to the VZV latency-associated transcript (VLT) and ORF63[7]. VLT is a polyadenylated RNA
79 comprising five exons that lie partially antisense to VZV ORF61, the infected cell
80 polypeptide 0 (ICP0) homologue conserved among αHV. Based on genomic location and
81 expression pattern, VLT is considered a homologue of the latency-associated transcripts
82 (LATs) encoded by all other well-studied neurotropic αHVs[8]. While VLT is the most
83 prevalent and abundant VZV transcript expressed in human TGs, lower levels of ORF63
84 RNA have also been reported in up to 70% of examined latently VZV-infected ganglia[7,9].
85 This apparent expression of two distinct viral transcripts during latency is unique among
86 well-studied αHV. Expression levels of VLT and ORF63 transcripts correlate significantly[7],
87 suggesting co-regulated expression of both transcripts during *in vivo* latency, and that

these transcripts and/or their encoded proteins may play an important role in the VZV latency and reactivation cycle. VLT is expressed during both latent and lytic VZV infection[7]. Intriguingly, VLT isoforms expressed during lytic VZV infection differ extensively from the latent VLT isoform in that they contain additional upstream exons and show evidence of alternative splicing by exon skipping or intron retention[7]. Furthermore, a long-read cDNA sequencing approach recently reported the presence of lytic VLT isoforms splicing into ORF63 during lytic VZV infection[10], raising the possibility that single transcripts may link the VLT and ORF63 loci.

Here, we set out to characterize the expression patterns and functional importance of VLT and ORF63 during lytic and latent infections. We applied direct RNA sequencing (dRNA-seq) on nanopore arrays[11] to examine lytically VZV-infected epithelial cells and discovered a novel set of VLT-ORF63 fusion transcripts, which are also present in latently VZV-infected human TG and our recently improved *in vitro* VZV human neuronal latency model based on human induced pluripotent stem cell (iPSC)-derived sensory neurons (HSN) [7,12].

RESULTS

Identification of multiple VLT-ORF63 fusion transcripts in lytically VZV-infected cells.

Sequencing of full-length RNAs, including direct RNA sequencing (dRNA-Seq), is particularly useful for disentangling complex loci at which multiple RNA isoforms overlap[13,14]. dRNA-Seq analysis of lytically VZV-infected human retina epithelial (ARPE-

19) cells identified numerous VLT isoforms, many of which utilized one or more major upstream exons, designated A, B, and C, upstream of the core VLT region (exon 1-5) that defines the latent isoform (**Fig. 1a**)[7]. We additionally identified several relatively abundant transcripts that spanned the VLT and ORF63 loci, hereafter referred as VLT-ORF63 fusion transcripts (**Fig. 1a**). Two major VLT-ORF63 isoforms (i.e. VLT-ORF63a and VLT-ORF63b) represent alternatively spliced variants of a lytic VLT isoform composed of the VLT core region, an additional upstream exon (A, B or C) and the complete ORF63 transcript. VLT-ORF63a and VLT-ORF63b differ from each other by skipping or retention of VLT exon 5, respectively. Both isoforms use a splice acceptor site located 71 nucleotides (nt) upstream of the ORF63 coding sequence (CDS), located within the 5'-untranslated region (UTR) of canonical ORF63[15,16]. A third major isoform (VLT-ORF63c) utilizes a unique transcription start site (TSS), not used by any of the other lytic VLT isoforms, proximal to exon 5 (**Fig. 1a**)[7].

To investigate the effect of cell type on the expression patterns of VLT, VLT-ORF63 and ORF63 during VZV infection, we assayed our *in vitro* HSN model that supports both lytic and latent VZV infection[12]. The low yields of viral RNA obtained from infected HSN cultures necessitated the use of nanopore cDNA sequencing (cDNA-Seq) rather than dRNA-Seq. Notably, the same VLT and VLT-ORF63 isoforms were detected in lytically VZV-infected HSN and ARPE-19 cells by both nanopore sequencing (**Fig. 1a**) and RT-qPCR (**Fig. 1b**) using primer sets spanning VLT-ORF63 isoform-defining exons (**Supplementary Fig. 1** and **Supplementary Table 1**). Collectively, these data indicate that identical repertoires

of VLT and VLT-ORF63 isoforms are expressed during lytic VZV infection in human sensory neurons and epithelial cells.

VLT-ORF63 explains co-regulated VLT and ORF63 transcription in latently VZV-infected human TG.

Detailed RT-qPCR was performed on four human TG specimens to determine whether ORF63 RNA detected in latently VZV-infected TG is derived from canonical ORF63 or VLT-ORF63s (**Supplementary Table 2**). Consistent to our earlier study[7], VLT was detected in all TG analyzed while ORF63 CDS region was detected in 3 of 4 specimens (**Fig. 2a**). No transcripts were detected using primer set ORF63UTR (**Supplementary Fig. 1**), which targets the 5' UTR of canonical ORF63 that is absent in all VLT-ORF63 transcripts. However, splice junction usage between VLT exon 4 or 5 and ORF63 was detected in all ORF63 CDS^{pos} TGs (**Fig. 2a**).

We next performed multiplex fluorescent *in situ* hybridization (mFISH) using VLT- and ORF63-specific probes to simultaneously profile VLT, VLT-ORF63 and ORF63 RNA expression in the same TG section. During lytic infection in HZ skin biopsies (**Fig. 2b, lower panels**) and ARPE-19 cells (**Supplementary Fig. 2a**), VLT and ORF63 ISH signal showed partial co-localization within the nucleus and largely divergent localization within the cytoplasm of VZV-infected cells. Analysis of seven additional human TGs (**Supplementary Table 3**) confirmed that VZV-infected neurons expressed nuclear VLT RNA (**Fig. 2b, middle panels**) or co-expressed nuclear VLT and ORF63 RNA ISH signal (**Fig. 2b, upper panels**). Notably, both RNAs co-localized in the vast majority of neurons (i.e.

4-11 neurons/section, present in all 7 TGs analyzed). Only a small number of neurons, 4 neurons in total and in just 2 of 7 TGs analyzed, yielded staining that showed both RNAs as distinct puncta (**Supplementary Fig. 2b**). Co-localization of VLT and ORF63 RNA ISH signal during latency provides further support for the presence of VLT-ORF63 fusion transcripts in human TG.

To further characterize and differentiate VLT, VLT-ORF63, and ORF63 transcripts in human TGs, 5'-RACE analysis was performed on pooled poly(A)-selected RNA collected from 3 TGs with detectable VLT-ORF63 transcripts (i.e. TG 2-4 in **Fig. 2a**). The VLT-specific reverse primers (VLTexon4R104361 and VLTexon5R104799 in **Fig. 2c** and **Supplementary Table 4**) identified two alternative TSS located 4 nt upstream and 21 nt downstream of VLT exon 1 (**Fig. 2c, blue arrows**), and detected only the core VLT with no alternatively spliced isoforms. The primers specifically binding to the ORF63 CDS (ORF63R622 and ORF63R805 in **Fig. 2c** and **Supplementary Table 4**) identified only two VLT-ORF63 isoforms of with alternative splicing donor sites located in VLT exons 4 and 5, respectively (**Fig. 2c**). Note that these VLT-ORF63 isoforms are identical to VLT-ORF63a and VLT-ORF63b isoforms expressed during lytic VZV infection, except for the unique 5' ends that discriminate latent from lytic VLT variants (**Fig. 1a**). Importantly, the TSS for all RNAs containing ORF63 sequence in human TG were located close to VLT exon 1 and were part of the VLT-ORF63 fusion transcript (**Fig. 2c, green arrows**), while no canonical ORF63 transcripts were detected. Collectively, these results implicate that most – if not all – ORF63 RNA detected in latently VZV-infected human TG is attributed to VLT-ORF63 transcript expression.

Protein coding potential differs between VLT-ORF63 transcript isoforms.

In silico translation of the two major VLT-ORF63 isoforms, VLT-ORF63a and VLT-ORF63b, predicted novel proteins (**Fig. 3a** and **Supplementary Fig. 3**), whereas VLT-ORF63c (**Fig. 1a**) appears to encode solely canonical ORF63 protein (pORF63). VLT-ORF63a encodes a putative in-frame fusion protein called pVLT-ORF63. The pVLT-ORF63 is predicted to 421 amino acids (aa) in length, comprising partial pVLT (aa 1-119) and the canonical pORF63 (278 aa) linked together by 24 aa polypeptide (GFVRFITRQRRVGFKGKGYYGPKD) encoded within the partial 5'-UTR of ORF63 (**Fig. 3a**). The VLT-ORF63b isoform is predicted to encode two separate proteins: complete pVLT (136 aa) and an N-terminally extended 336 aa pORF63 protein variant (pORF63-N+). pORF63-N+ includes an N-terminal 88 aa polypeptide, the first 64 aa of which are translated from VLT exons 4 and 5, but out-frame with pVLT, and the same 24 aa linker polypeptide of pVLT-ORF63 encoded from the partial 5'-UTR of ORF63 (**Fig. 3a**).

The protein coding capabilities of the VLT-ORF63 isoforms were examined by immunoblotting of ARPE-19 cells transfected with plasmids expressing VLT-ORF63a and VLT-ORF63b, and ORF63 for comparison, as well as in lytically VZV-infected ARPE-19 cells using antibodies raised against parts of pVLT and pORF63 (**Supplementary Fig. 4**). The anti-pVLT antibody (Ab) was raised against the first 19 aa of pVLT[7], being part of both pVLT and pVLT-ORF63. The anti-pORF63 Ab was raised against whole pORF63[7], recognizing pVLT-ORF63, pORF63-N+ and pORF63. Translation of all predicted proteins from each plasmid was confirmed in transfected ARPE-19 cells and both pVLT-ORF63 and

pORF63-N+ were readily detected in the context of lytic VZV infection (**Supplementary Fig. 4**).

Next, we assayed the cellular localization of protein expression by immunofluorescence. In transfected cells, pORF63 was detected in the nucleus and particularly in the cytoplasm, whereas pVLT-ORF63 predominantly localized in the nucleus (**Fig. 3b**). The same result was obtained with an antibody (anti-pVLT-ORF63 Ab) specific for the 24 aa linker region present exclusively in the VLT-ORF63 fusion proteins. Cells transfected with the VLT-ORF63b vector, encoding pVLT and fusion protein pORF63-N+, resulted in nuclear and cytoplasmic pVLT but undetectable pORF63-N+ expression (**Fig. 3b**). In lytically VZV-infected ARPE-19 cells, pVLT-ORF63 localized to the nucleus and cytoplasm, as demonstrated by immunofluorescent staining with antibodies against pVLT-ORF63, pVLT and pORF63 (**Fig. 3c**). Finally, we showed pVLT-ORF63 expression in HZ skin biopsies that specifically localized in the cytoplasm of VZV-infected pORF63^{pos} keratinocytes (**Fig. 3d**). Thus, pVLT-ORF63 and/or pORF63-N+ are expressed in VZV-infected cells *in vitro* and *in vivo*.

Treatment with JNK activator promotes VLT-ORF63 transcription in latently VZV-infected sensory neurons.

We next used our *in vitro* VZV sensory neuronal latency model[12] to examine transcription patterns across the VLT and ORF63 loci by RT-qPCR during latency and reactivation. Consistent with VZV latency in human TG, VLT was readily detectable in latently VZV-infected HSN, while no other tested viral immediate early (IE), early (E) or late (L)

transcripts were detected (**Fig. 4a**). Notably, we detected neither ORF63 (CDS and 5'-UTR) nor any of the VLT-ORF63 isoforms (**Fig. 4a**), whose absence was seen only in small fraction of human TGs (**Fig. 2a** and reference[7]). 5'-RACE analysis of VLT and ORF63 loci on RNA extracted from latently VZV-infected HSN confirmed expression of core VLT isoform and usage of the two VLT TSS detected in human TG as well as a third TSS located 9 nt upstream of VLT exon 1 (**Fig. 2c, red arrows**), and the lytic VLT and VLT-ORF63 isoforms were not detected.

Similar to previously reported *in vitro* models for VZV latency using human embryonic stem cell (hESC)-derived neurons[17,18], induction of complete virus reactivation was relatively inefficient in our HSN model[12]. Complete reactivation was observed in 2 of 40 replicates, as demonstrated by the formation of infectious foci after transferring the HSN onto and co-culturing with ARPE-19 cells (**Fig. 4b, upper panel**), and associated with expression of all IE, E and L VZV transcripts tested in the HSN (**Fig. 4c, black circle**). Although no infectious virus was detected in 38 replicates (**Fig. 4b, lower panel**), low levels of multiple viral transcripts could be detected including VLT-ORF63a indicative of exit from latency (**Fig. 4c, while circle**). These data indicate that VLT expression is a hallmark of VZV latency in human sensory neurons *in vitro*, while VLT-ORF63s are induced in response to reactivation stimuli.

Given the critical role of JNK activation as a trigger of HSV-1 lytic gene expression during reactivation[19] as well as the importance of the JNK signal in VZV reactivation[20], we speculated that JNK activation may trigger VZV reactivation by inducing lytic gene expression. Latently VZV-infected HSN were treated with the JNK activator anisomycin,

241 a compound that also inhibits protein synthesis. VZV reactivation, as measured by
242 transferring HSN onto ARPE-19 cells for infectious focus forming assay, could not be
243 detected. However, anisomycin treatment consistently increased VLT expression and
244 induced expression of VLT-ORF63a and VLT-ORF63b (**Fig. 4d**). By contrast, anisomycin
245 treatment induced only limited expression of ORF4 (1 of 3 replicates) or ORF61 (2 of 3
246 replicates), while no lytic VZV gene transcription was detected following mock treatment
247 (**Fig. 4e**). Thus, anisomycin-mediated JNK activation and/or inhibition of protein
248 synthesis selectively and consistently induces transcription of VLT and both VLT-ORF63
249 isoforms in parallel with or prior to induction of IE gene transcription.
250
251 ***Ectopic VLT-ORF63a expression induces broad viral gene expression in the latently VZV-***
252 ***infected sensory neuron model.***
253 The anisomycin-induced VLT-ORF63 transcription suggest that these transcripts directly,
254 or their encoded proteins, contribute to VZV reactivation. To investigate whether VLT-
255 ORF63a or VLT-ORF63b alone can induce VZV reactivation, latently VZV-infected HSN
256 were transduced with replication-incompetent lentivirus vectors encoding ORF63, the
257 latent VLT-ORF63a and VLT-ORF63b isoforms, or an empty vector control. Ectopic gene
258 transcription and translation was confirmed in all transduced cell cultures (**Fig. 5** and
259 **Supplementary Fig. 5**). Both in the empty vector and ORF63-transduced cells,
260 endogenous VLT was detected by RT-qPCR at comparable level (**Fig. 5a, b**). Sporadic IE
261 and E gene, but no L gene transcription was detected in ORF63- and VLT-ORF63b-
262 transduced cells (**Fig. 5b, c**). Notably, transcription of VZV IE, E and L genes was

consistently induced by ectopic VLT-ORF63a expression in latently VZV-infected HSN (**Fig. 5d**). Consistent with the absence of ORF62 transcription, which encodes the major viral transactivator protein[21], no infectious VZV was recovered from VLT-ORF63a-transduced HSN cells. Given the differences in protein coding potential between the VLT isoforms and compared to canonical ORF63 (**Fig. 3a**), the pVLT-ORF63 fusion protein is potentially involved in the transition from latency to reactivation in our HSN VZV latency model.

DISCUSSION

VZV latency in human TG is characterized by detection of RNAs expressed from the VLT and occasionally the ORF63 locus, where expression levels of both transcripts correlated positively suggesting co-regulated transcription[7]. Here, we demonstrated that this pattern is best explained by co-expression of VLT and two VLT-ORF63 fusion transcripts, and not by expression of the canonical ORF63 transcripts independent of VLT. Further characterization of the VLT-ORF63 isoforms, expressed during both lytic and latent VZV infection, demonstrated that reactivation stimuli increase VLT and induce VLT-ORF63 expression in our *in vitro* VZV HSN latency model. Moreover, ectopic VLT-ORF63a expression induced broad viral lytic gene transcription in latently VZV-infected HSN, which is potentially mediated by the pVLT-ORF63 fusion protein.

Differential TSS usage of VLT between latently-VZV infected TGs and lytically VZV-infected epithelial cells[7] raises the question as to whether transcription of distinct VLT isoforms depends on infection phase or cell type. Here, we demonstrated that

transcription of specific VLT and VLT-ORF63 isoforms is determined by the infection phase rather than the cell type. While both lytic and latent transcript isoforms are predicted to encode the same protein(s), the extended 5'-UTR in the lytic VLT and VLT-ORF63 transcripts may confer new properties to the RNA. Alternative promoter usage of viral genes between distinct but continuous infection phases has been implicated as a switching mechanism of latency and lytic infection among herpesviruses[22-24], and may impact on the localization and/or function of both type of VZV transcripts at different infection phases.

Transcriptional profiling of reactivating neurons in our *in vitro* HSN latency model revealed the presence of multiple viral transcripts of all kinetic classes, including the VLT-ORF63 RNAs. By contrast, when attempting to induce reactivation through anisomycin-mediated activation of JNK signaling, previously shown to be required for VZV reactivation and replication[20], only VLT-ORF63 transcription was consistently induced along with higher expression levels of VLT. This provides a favorable explanation as to how VZV initially reactivates from latency. As a counterpoint, we do note the limitations imposed by using anisomycin to show a direct link between JNK signaling and complete reactivation. Specifically anisomycin inhibits protein synthesis and just 1 hr exposure to anisomycin induces a terminal decline of neuronal cultures with death occurring within 14 days of treatment, regardless of whether cells were latently VZV-infected or not. Hence, further studies are needed to delineate the mechanisms by which JNK signaling regulates VZV gene expression and reactivation in latently VZV-infected HSN.

306 The VLT-ORF63a, but not VLT-ORF63b isoform induced broad lytic viral gene
307 transcription in latently VZV-infected HSN cultures. While these two isoforms differ only
308 by the partial presence/absence of VLT core exon 5, only VLT-ORF63a encodes for the
309 pVLT-ORF63, suggesting that the encoded protein and not the transcript itself regulates
310 transcription of VZV genes. Canonical pORF63 has been reported to both positively and
311 negatively affect VZV gene transcription during lytic infection[25,26], depending on its
312 phosphorylation status and cell type analyzed[27]. Here, we showed that pORF63 induces
313 expression of IE gene ORF61 encoding a promiscuous transactivator protein[28] and the E
314 gene ORF16, but not any of the other analyzed VZV IE, E or L genes in our *in vitro* HSN
315 latency model. By contrast, pVLT-ORF63 induced expression of multiple VZV genes of all
316 kinetic classes. Overall, the data suggest a key role for pVLT-ORF63 in the initiation of
317 VZV reactivation and emphasize the importance of uncharacterized cellular factors
318 and/or other viral factors (e.g. expression of the major viral transcriptional activator
319 pORF62, which is consistently absent in VLT-ORF63a transduction) that are required for
320 complete VZV reactivation for future studies.

321 HSV reactivation has been proposed to be consisted with two distinct but
322 continuous waves of lytic gene transcription. The first wave designated as animation[29]
323 or Phase I[30,31] is characterized by generalized viral gene derepression[30,32], in contrast the
324 second wave (Phase II) is identical to the cascade observed during acute infection.
325 Transition from latency to Phase I and Phase I to Phase II might work as checkpoints
326 whether to lead complete reactivation or to halt reactivation and re-enter latency[30].
327 While we do not know whether animation/Phase I occurs during VZV reactivation, broad

328 transcription of viral genes of all kinetic classes was induced by reactivation stimuli,
329 occasionally leading to complete reactivation in our *in vitro* HSN latency model. Notably,
330 our data demonstrates that broad VZV transcription is initiated by VLT-ORF63
331 transcription/pVLT-ORF63 translation, unlike Phase I of HSV reactivation for which no
332 viral initiator has been proposed to drive HSV gene expression. Thus, there might be
333 critical differences between the mechanism(s) governing HSV and VZV latency and
334 reactivation.

335 Taken together, our discovery of the VLT-ORF63 fusion transcripts in VZV-infected
336 human TG and the ability of the encoded pVLT-ORF63 fusion protein to act as an initiator
337 of viral gene expression during reactivation in our *in vitro* HSN latency model provides
338 critical new insights into how VZV latency and reactivation are governed. Further studies
339 using the HSN VZV latency model, combined with careful analyses of human ganglia,
340 provides a new platform to dissect the cellular and viral molecular mechanisms
341 controlling VZV latency and reactivation. VZV is the only human herpesvirus for which
342 vaccines are licensed. However, the live-attenuated varicella vaccine establishes latency
343 and may reactivate to cause disease, while adjuvanted recombinant zoster vaccine is
344 highly effective against HZ prevention but not suited for childhood varicella vaccination.
345 The discovery of VLT-ORF63 and its role in reactivation provides new insight that will
346 inform efforts to improve varicella vaccines.
347

METHODS

Human clinical specimens.

Human TG specimens were obtained (**Supplementary Tables 1 and 2**) from the Netherlands Brain Bank (Netherlands Institute for Neuroscience; Amsterdam, the Netherlands). All donors had provided written informed consent for brain autopsy and the use of material and clinical information for research purposes. All study procedures were performed in compliance with relevant laws in The Netherlands and Japan, institutional guidelines approved by the local ethical committee (VU University Medical Center, Amsterdam, project number 2009/148, and Kobe University, Kobe, project number 170107) and in accordance with the ethical standards of the Declaration of Helsinki. TG biopsies were either formalin-fixed and paraffin-embedded (FFPE) for *in situ* analysis or snap-frozen in liquid nitrogen and stored at -80°C for nucleic acid extraction. FFPE skin punch biopsies of one healthy control subject and two herpes zoster skin lesions were obtained for diagnostic purposes. According to the institutional "Opt-Out" system (Erasmus MC, Rotterdam, the Netherlands), which is defined by the National "Code of Good Conduct" [Dutch: Code Goed Gebruik, May 2011], the surplus human herpes zoster FFPE tissues were available for the current study.

Cells.

Human iPSC-derived sensory neuron (HSN) progenitors (Axol Bioscience) were plated on a 24-well plate (1 x 10^5 cells/well), CELLview Slide (Greiner Bio-One) (1 x 10^4 cells/well)

or a microfluidic platform (7.5 x 10^4 cells/sector) in Neuronal Plating-XF Medium (Axol Bioscience). Fabrication of a microfluidic platform was previously described[33]. Prior to plating the HSN progenitors, a plate, slide or microfluidic platform was coated with poly-L-ornithine (Sigma-Aldrich) (20 µg/mL) or poly-D-lysin (Sigma-Aldrich) (200 µg/mL) in molecular grade water at room temperature overnight, washed with distilled water twice and coated with Matrigel (Corning) (1 µg/mL) in Knockout DMEM/F-12 medium (Thermo Fisher Scientific) for 2 hr at room temperature following overnight incubation at 37°C in a humified 5% CO_2 incubator. At 1 day after plating, the medium was replaced to the complete maintenance medium consisted with Neurobasal Plus Medium, B-27 Plus Supplement (2% [vol/vol]), N2 Supplement (1% [vol/vol]), GlutaMAX-I (2 mM) (Thermo Fisher Scientific), ascorbic acid (200 µM; Sigma-Aldrich), GDNF (25 ng/mL), NGF (25 ng/mL), BDNF (10 ng/mL) and NT-3 (10 ng/mL) (Peprotech) for sensory neuronal maturation. Two days after the plating the HSN progenitors, cells were treated with the complete maintenance medium with mitomycin C (2.5 µg/mL; Nacalai Tesque, Inc.) for 2 hr to eliminate proliferating cells, washed with the complete medium twice and culture in the complete maintenance medium at least 7 weeks with replacing half the volume of culture with the fresh medium every 4 days. During maturation in the microfluidic platform, culture medium level in the axonal compartment was kept higher than that in the somal compartment to prevent cell migration to the axonal compartment. The maturation of sensory neurons was characterized previously[12]. Human retinal pigmented epithelium ARPE-19 cells (American Type Culture Collection [ATCC] CRL-2302) were maintained in DMEM/F-12+GlutaMAX-I (Thermo Fisher Scientific)

supplemented with heat-inactivated 8% FBS (foetal bovine serum; Sigma-Aldrich). Human embryonic kidney (HEK) 293T cells (ATCC CRL-3216) were cultured in DMEM+GlutaMAX-I (Thermo Fisher Scientific) supplemented with heat-inactivated 8% FBS.

VZV infections.

VZV strain pOka (parental Oka) was maintained in and the cell-free virus was prepared from ARPE-19 cells as described previously for human embryonic lung fibroblast MRC-5 cells[34]. For lytic infection in ARPE-19 cells, cells were plated on 12-well plate at a density of 1 x 10^5 cells/well 2 days before infection, infected with the cell-free virus (3 x 10^3 pfu [plaque-forming unit] to 1 well) for 1 hr in 500 µL medium, washed with the medium twice and cultured for 4 days. For lytic infection for HSN, cells were maturated as described above, infected with the cell-free virus (4 x 10^3 pfu to 1 well) at 52 days after maturation for 2 hrs in 400 µL medium, washed with the medium twice, treated with low pH buffer (40 mM sodium citrate, 10 mM potassium chloride, 135 mM sodium chloride [pH 3.2]) for 30 seconds (sec), washed with the medium once and cultured for 2 weeks to obtain efficient lytic infection as described[12].

For *in vitro* VZV latency, the method was established previously for human embryonic stem cell-derived neurons[18] and applied for HSN[12]. Briefly, HSN were maturated on a microfluidic platform for 54 days and infected via axonal chamber with 10 µL of the cell-free virus (4 x 10^4 pfu/mL titrated on ARPE-19 cells) in 20 µL total volume. After 2 hr infection, inoculum was removed, and axons were treated with the low pH

buffer for 30 sec, washed with the medium and cultured for 2 weeks. To reactivate VZV from sensory neuronal latency, GDNF, NGF, BDNF and NT-3 were depleted from and anti-NGF polyclonal antibody (50 µg/mL) was added to the complete maintenance medium, and cultures were maintained for 2 weeks. For chemical induced reactivation, latently VZV-infected HSN was treated with JNK activator, anisomycin (20 µg/mL) or solvent control (DMSO [dimethyl sulfoxide]) for 1 hr from both axonal and somal compartment, washed with the medium twice and cultured in the complete maintenance medium without GDNF, NGF, BDNF and NT-3 for 1 week. For VZV gene transduction, VZV-latently infected HSN was transduced by lentivirus vector for 2 hr from somal compartment with mixing by pipetting at 30 minutes (min) and 1.5 hr after transduction, cultured overnight and replaced the medium in both somal and axonal compartment with the fresh complete maintenance medium without GDNF, NGF, BDNF and NT-3 for 2 weeks. The complete reactivation was confirmed by the formation of infectious foci after transferring the HSN onto and co-culturing with ARPE-19 cells for 7 days as described below.

DNA, RNA and cDNA.

DNA and RNA were isolated from human TGs (n = 4) (**Supplementary Table 2**) as described previously[7]. DNA and RNA from VZV-infected ARPE-19 cells or HSN were isolated as described previously[7] with slight modifications using the FavorPrep Blood/Cultured Cell Total RNA Mini Kit (FAVORGEN BIOTECH) in combination with the NucleoSpin RNA/DNA buffer set (Macherey-Nagel). DNA was first eluted from the

column in 80 µL DNA elution buffer, the column was treated with recombinant DNase I (20 units/100 µL; Roche Diagnostics) for 30 min at 37°C and RNA was eluted in 50 µL nuclease free water. RNA was directly treated with Baseline-ZERO DNase (2.5 units/50 µL; Epicentre) for 30 min at 37°C (all the RNA), and further purified by Dynabeads mRNA purification kit (Thermo Fisher Scientific) (TG RNA) or enriched by Agencourt RNAClean XP (Beckman Coulter) (i*n vitro* latency RNA). cDNA was synthesized with 12 µL of RNA and anchored oligo(dT)$_{18}$ primer in a 20 µL reaction using the Transcriptor First Strand cDNA synthesis kit at 55°C for 30 min for reverse transcriptase reaction (Roche Diagnostics).

Quantitative PCR and 5'-RACE analysis.

DNA or cDNAs were subjected to quantitative PCR (qPCR) using KOD SYBR qPCR Mix (TOYOBO) in the StepOnePlus Real-time PCR system (Thermo Fisher Scientific) (1 µL of DNA or cDNA per 10 µL reaction in duplicate). All the primer sets used for qPCR (**Supplementary Table 1**) were first confirmed for the amplification rate (98-100%) using 10-10^6 copies (10-fold dilution) of pOka-BAC genome or VLT-ORF63 plasmids and the lack of non-specific amplification using water. Due to the partially antisense nature of VLT via exon 3 and exon 4 against ORF61, a primer pair of exons 3 and 4 detected both VLT and ORF61, thus a primer pair of exons 2 and 4 was used for lytic infection instead a primer pair of exons 3 and 4 used for *in vivo* and *in vitro* latency in which ORF61 is absent. The qPCR program is as follows; 95°C for 2 min (1 cycle), 95°C for 10 sec and 60°C 15 sec (40 cycles), and 60 to 95°C for a dissociation curve analysis to discriminate non-specific signal

458 if any. Data is presented as relative transcription level of VZV gene to cellular beta-actin
459 defined as $2^{-(\text{Ct-value VZV gene} - \text{Ct-value beta-actin})}$.

460 5'-RACE analysis was performed using SMARTer RACE 5'/3' kit and In-Fusion HD
461 Cloning kit according to the manufacturer's instructions with slight modifications
462 (Clontech). 5'-RACE ready cDNA was synthesized from purified mRNA (TG) or total RNA
463 (HSN) with SMARTerIIA Oligonucleotide and 5'-RACE CDS Primer A. KOD FX Neo PCR
464 system (TOYOBO) was used for 5'-RACE PCR and the program was 1 cycle of 94°C for 2
465 min and 30 cycles of 95°C for 10 sec and 68°C for 1 min. Initial PCR was performed by
466 Universal Primer Mix (a mixture of Universal Primer Long and Universal Primer Short)
467 and InFusionVLTexon5R104799 for VLT or InFusionORF63R805 for VLT-ORF63 fusions.
468 Nested PCR, if necessary, was carried out using Universal Primer Long and
469 InFusionVLTexon4R10361 for VLT or InFusionORF63R622 for VLT-ORF63 fusions. The 5'-
470 RACE PCR products were cloned into linearized pRACE cloning vector and sequenced by
471 M13forward or M13reverse on the ABI Prism 3130 XL Genetic Analyzer using the BigDye
472 v3.1 Cycle Sequencing Kit (Thermo Fisher Scientific). All the primers used for 5'-RACE
473 analysis are listed in **Supplementary Table 4**.
474
475 ***Direct RNA sequencing and cDNA sequencing on nanopore array.***
476 Direct RNA sequencing libraries were generated from 117 - 153 ng of poly(A) RNA,
477 isolated using Dynabeads mRNA purification kit. Isolated poly(A) RNA was subsequently
478 spiked with 0.5 µl of a synthetic Enolase 2 (ENO2) calibration RNA (Oxford Nanopore
479 Technologies Ltd.) and sequenced on a MinION MkIb with R9 flow cells (Oxford

Nanopore Technologies Ltd.) for 40 hr, as previously described[14]. cDNA sequencing libraries were generated from 1 ng of poly(A) RNA, isolated using Dynabeads mRNA purification kit using cDNA-PCR Sequencing kit (SQK-PCS109) (Oxford Nanopore Technologies Ltd.) and sequenced on a MinION MkIb with R9 flow cells for 40 hr. Following basecalling with Albacore, only the reads in the pass folder were used. Error-correction was performed using proovread as described previously[14]. Nanopore read data were aligned to the VZV strain dumas genome (X04370.1) using MiniMap2[35] and parsed using SAMtools[36] and BEDTools[37].

Multiplex fluorescent RNA in situ hybridization in human cadaveric TG.

FFPE latently VZV-infected human TG (n = 7) (**Supplementary Table 3**), human zoster skin biopsies and lytically VZV-infected ARPE-19 cells were analyzed by multiplex fluorescent *in situ* hybridization (mFISH) using the RNAScope Multiplex Fluorescent Reagent Kit v2 (Advanced Cell Diagnostics) according to the manufacturer's instructions. Briefly, deparaffinized 5 µm-thick tissue sections were incubated with probes directed to ORF63 and VLT exons 2 – 5. RNA integrity and mFISH specificity were demonstrated by staining TGs for ubiquitously expressed cytoplasmic transcript ubiquitin C, nuclear transcript MALAT1 (positive controls) and bacterial gene DAPB (negative control probe) (**Supplementary Fig. 2C**). Probes were designed by Advanced Cell Diagnostics. Sections were mounted with Prolong Diamond antifade mounting medium and confocal microscopic analysis was performed on a Zeiss LSM 710 confocal microscope, as described[38].

Replication incompetent lentivirus vectors.

VZV genes, ORF63, VLT-ORF63a or VLT-ORF63b were amplified by PCR of cDNA from VZV pOka-infected ARPE-19 cells. The PCR product was digested with SalI restriction enzyme and cloned into CS-CA-MCS plasmid (Riken BioResource Research Center) via SalI site (ORF63) or directly cloned into linearized CS-CA-MCS (VLT-ORF63a and VLT-ORF63b) using In-Fusion HD Cloning kit according to the manufacturer's instruction (Clontech). The primer sets used for cDNA cloning into the CS-CA-MCS plasmid are listed in **Supplementary Table 4**. HEK293T cells (4 x 10^6 cells) were plated onto a 10 cm dish, transfected with CS-CA-MCS or CS-CA-VZV (20 µg) and packaging plasmids, pCAG-HIVgp (5 µg) and pCMV-VSV-G-RSV-Rev (5 µg) (Riken BioResource Research Center) using PEImax solution (60 µL) (Polysciences) prepared in KnockoutDMEM/F-12 (500 µL) at 6 hr post plating and cultured overnight in 8% CO_2 incubator in 10 mL DMEM+GlutaMAX-I with heat-inactivated 8% FBS. Whole culture medium was change with the fresh medium at 16 hr after transfection and cells were cultured for another 48 hr. Supernatant (20 mL) were filtrated through 0.45 µm syringe filter (Pall), mixed with 5 mL of PEG6000 (50% [wt/vol] in PBS), 1.7 mL of 5 M NaCl and 2.6 mL of PBS, and rotated in a 50 mL conical tube at 4°C at least 8 hr. After centrifugation at 7,000 x g for 10 min, supernatant was removed, pellet was resuspended in 300 µL of KnockoutDMEM/F-12, aliquoted out in 4 tubes and stored at -80°C until use. Quantity of each replication incompetent lentivirus vector was measured by qPCR of cDNA synthesized with random hexamer from genomic RNA packaged in enriched pseudo virion using the primer set, CSCA1831F and

524 CSCA1969R (**Supplementary Table 1**) detecting upstream promoter region in CS-CA-MSC
525 plasmid and equal amount of virus were used for transductions.
526
527 ***Antibodies.***
528 Chicken polyclonal antibody (pAb) against 24 aa linker peptide
529 (GFVRFITRQRRVGFKGKGYYGPKD) of pVLT-ORF63 fusion protein, anti-pVLT-ORF63 pAb
530 was generated and purified through an immunogen conjugated peptide column (Cosmo
531 Bio). Rabbit anti-pVLT pAb, rabbit anti-pORF63 pAb[7], mouse anti-pORF63 monoclonal
532 antibody (mAb)(clone VZ63.08)[39], and mouse anti-glycoprotein E (gE) mAb[40] were
533 described previously. Anti-alpha tubulin mAb (clone B-5-1-2; Sigma-Aldrich) and sheep
534 anti-NGF pAb (EMD Millipore) are commercially available. Alexa Fluor 488- or Alexa
535 Fluor 647-conjugated donkey anti-mouse IgG, Alexa Fluor 594-conjugated donkey anti-
536 rabbit IgG (Thermo Fisher Scientific) and Alexa Fluor 488-conjugated donkey anti-
537 chicken IgY (Jackson ImmunoResearch Laboratories) were used for secondary Abs for
538 indirect immunofluorescent assay. Anti-mouse IgG HRP-linked Whole Ab Sheep or anti-
539 rabbit IgG HRP-linked Whole Ab Donkey (GE Healthcare Bio-Sciences) were used as
540 secondary Abs for immunoblotting.
541
542 ***Immunofluorescent staining, confocal microscopy, infectious foci staining and***
543 ***immunoblotting.***
544 Cells on CELLview slide were fixed with 4% (vol/vol) paraformaldehyde (PFA)/PBS
545 (Nacalai Tesque, Inc.) at room temperature for 20 min, permeabilized with 0.1% Triton

546 X-100/4% PFA/PBS at room temperature for 20 min, and incubated with human Fc
547 receptor blocking solution (5% FBS/PBS containing 10% of Clear Back [MBL]) at room
548 temperature for 1 hr. Cells were stained with the primary Abs diluted in a solution (5%
549 FBS/PBS) overnight at 4°C (1:100 for anti-pVLT pAb, anti-pVLT-ORF63 pAb and anti-
550 pORF63 mAb, 1:300 for all Abs against neuronal markers, 1:500 for anti-pORF63 pAb),
551 washed with 0.1% Tween 20/PBS (PBS-T) for 5 min 3 times, stained with the secondary
552 Abs (1:300) diluted in 5% FBS/PBS at room temperature for 1 hr, washed with PBS-T for
553 5 min 3 times, covered with VECTASHIELD Vibrance Antifade Mounting Medium with
554 DAPI (Vector Laboratories) and imaged by an FV1000D confocal microscopy (Olympus).
555 Deparaffinized and rehydrated 5 μm FFPE sections of human herpes zoster skin
556 lesions and healthy control skin were subjected to heat-induced antigen retrieval with
557 citrate buffer (pH=6.0), blocked and incubated with mouse anti-VZV pORF63 (1:1,500
558 dilution; kindly provided by Dr. Sadzot-Delvaux; Liege, Belgium[41]), chicken anti-pVLT-
559 ORF63 (1:100 dilution) overnight at 4°C. Sections were subsequently incubated with
560 Alexa Fluor 488- and Alexa Fluor 594-conjugated goat-anti-mouse and goat-anti-chicken
561 secondary antibodies (all 1:250 dilution) and sections were mounted with Prolong
562 Diamond antifade mounting medium with DAPI. Confocal microscopic analysis was
563 performed as described[38].
564 To visualize infectious foci on ARPE-19 cells, cells were fixed with 4% PFA/PBS,
565 stained with anti-gE mAb (1 : 10 dilution in PBS), followed by anti-mouse IgG HRP-linked
566 whole Ab sheep (1:5,000 dilution in PBS), and reacted with 3, 3', 5, 5'-
567 tetramethylbenzidine-H peroxidase substrate (Moss, Inc.).

Cells were incubated in RIPA lysis buffer (0.01 M Tris-HCl [pH 7.4], 0.15 M NaCl, 1% sodium deoxycholate, 1% Nonidet P-40 and 0.1% SDS) on ice for 15 min, sonicated in a water bath for 10 min, centrifuged at 20,000 x g for 15 min. Supernatant was boiled with LDS Sample Buffer (4X) and Sample Reducing Agent (10X) at 100°C for 5 min (Thermo Fisher Scientific). Proteins were separated on 4-12% Bis-Tris Plus Gel in MES SDS Running Buffer (200 V, 25 min), transferred onto PVDF membrane (0.2 µm) using Mini Blot Module (20V, 1 hr) in Bolt Transfer Buffer containing 10% methanol and 0.1% Bolt Antioxidant (Thermo Fisher Scientific). The membrane was blocked in a blocking buffer (5% [wt/vol] skimmed milk/0.1% Tween 20/PBS) at room temperature for 1 hr, stained with primary Abs diluted in the blocking buffer (1:1,000 for anti-pVLT pAb, 1:6,000 for anti-pORF63 pAb and 1:10,000 for anti-alpha tubulin mAb) overnight at 4°C, washed with PBS-T for 5 min 3 times, stained with the secondary Abs diluted in the blocking buffer (1:3,000) at room temperature for 30 min, and washed with PBS-T for 5 min 3 times and PBS briefly once. Signals were visualized by Chemi-Lumi One Super Nacalai Tesque, Inc.) and captured using LAS4000mini (GE Healthcare Bio-Sciences). A membrane stained with anti-pVLT pAb was stripped by WB Stripping Solution Strong in accordance with the manufacturer's manual (Nacalai Tesque, Inc.) and reprobed with anti-alpha-tubulin mAb.

Data Availability

Basecalled fast5 nanopore dRNA- and cDNA-Seq datasets generated as part of this study can be downloaded from the European Nucleotide Archive (ENA) under the following

590 study accession: PRJEB36978. The authors declare that all other data supporting the
591 findings of this study are available within the article and its Supplementary Information
592 files, or are available from the authors upon request.
593
594 **Acknowledgements**
595 We are grateful to Yasuko Mori for use of laboratory equipment, Angus C. Wilson and
596 Ian Mohr for critical reading of the manuscript. This work was supported by the Takeda
597 Science Foundation, Daiichi Sankyo Foundation of Life Science, Japan Society for the
598 Promotion of Science (JSPS KAKENHI JP17K008858, JP16H06429 and JP16K21723) and
599 the Ministry of Education, Culture, Sports, Science and Technology (MEXT KAKENHI
600 JP17H05816) (T. S.). A. V. is supported by the NIH NINDS (R21NS107991). J. B. receives
601 funding from the UCL/UCLH NIHR Biomedical Research Centre. S. J. and T. L. R. are
602 supported by “Strengthening the capacity of CerVirVac for research in virus immunology
603 and vaccinology”, grant no. KK.01.1.1.01.0006, awarded to the Scientific Centre of
604 Excellence for Virus Immunology and Vaccines and co-financed by the European
605 Regional Development Fund. The funders had no role in study design, data collection,
606 and interpretation, or in the decision to submit the work for publication.
607
608

609 **REFERENCES**

610

611 1. Cohen, J. I. in *Human Herpesviruses: Biology, Therapy, and Immunoprophylaxis*
612 (eds. Arvin, A. M. et al.) (Cambridge University Press, 2007).
613 2. Gershon, M. & Gershon, A. Varicella-Zoster Virus and the Enteric Nervous System.
614 *J INFECT DIS* **218,** S113–S119 (2018).
615 3. Gershon, A. A. *et al.* Varicella zoster virus infection. *Nat. Rev. Dis. Primers* **1,** 15016
616 (2015).
617 4. Abendroth, A. & Arvin, A. M. in *Human Herpesviruses: Biology, Therapy, and*
618 *Immunoprophylaxis* (eds. Arvin, A. M. et al.) (Cambridge University Press, 2007).
619 5. Tseng, H. F. *et al.* The epidemiology of herpes zoster in immunocompetent,
620 unvaccinated adults ≥50 years old: incidence, complications, hospitalization,
621 mortality, and recurrence. *J INFECT DIS* **57,** 1 (2019).
622 6. Chen, S. Y. *et al.* Incidence of herpes zoster in patients with altered immune
623 function. *Infection* **42,** 325–334 (2014).
624 7. Depledge, D. P. *et al.* A spliced latency-associated VZV transcript maps antisense
625 to the viral transactivator gene 61. *Nature Communications* **9,** 1167 (2018).
626 8. Depledge, D. P., Sadaoka, T. & Ouwendijk, W. J. D. Molecular Aspects of Varicella-
627 Zoster Virus Latency. *Viruses* **10,** 349 (2018).
628 9. Ouwendijk, W. J. D. *et al.* Restricted varicella-zoster virus transcription in human
629 trigeminal Ganglia obtained soon after death. *Journal of Virology* **86,** 10203–
630 10206 (2012).

10. Prazsák, I. *et al.* Long-read sequencing uncovers a complex transcriptome topology in varicella zoster virus. *BMC Genomics* **19,** 873 (2018).

11. Garalde, D. R. *et al.* Highly parallel direct RNA sequencing on an array of nanopores. *Nat. Methods* **15,** 201–206 (2018).

12. Sadaoka, T. *et al.* Human stem cell derived sensory neurons are positioned to support varicella zoster virus latency. *bioRxiv* 1–35 (2020). doi:10.1101/2020.01.24.919290

13. Depledge, D. P., Mohr, I. & Wilson, A. C. Going the Distance: Optimizing RNA-Seq Strategies for Transcriptomic Analysis of Complex Viral Genomes. *Journal of Virology* **93,** 860 (2019).

14. Depledge, D. P. *et al.* Direct RNA sequencing on nanopore arrays redefines the transcriptional complexity of a viral pathogen. *Nature Communications* **10,** 754 (2019).

15. Kinchington, P. R., Vergnes, J. P., Defechereux, P., Piette, J. & Turse, S. E. Transcriptional mapping of the varicella-zoster virus regulatory genes encoding open reading frames 4 and 63. *Journal of Virology* **68,** 3570–3581 (1994).

16. Kost, R. G., Kupinsky, H. & Straus, S. E. Varicella-zoster virus gene 63: transcript mapping and regulatory activity. *Virology* **209,** 218–224 (1995).

17. Markus, A., Lebenthal-Loinger, I., Yang, I. H., Kinchington, P. R. & Goldstein, R. S. An In Vitro Model of Latency and Reactivation of Varicella Zoster Virus in Human Stem Cell-Derived Neurons. *PLoS Pathog* **11,** e1004885 (2015).

18. Sadaoka, T. *et al.* In vitro system using human neurons demonstrates that

varicella-zoster vaccine virus is impaired for reactivation, but not latency. *Proc Natl Acad Sci USA* **113,** E2403–12 (2016).

19. Cliffe, A. R. *et al.* Neuronal Stress Pathway Mediating a Histone Methyl/Phospho Switch Is Required for Herpes Simplex Virus Reactivation. *Cell Host Microbe* **18,** 649–658 (2015).

20. Kurapati, S. *et al.* Role of the JNK Pathway in Varicella-Zoster Virus Lytic Infection and Reactivation. *Journal of Virology* **91,** e00640–17 (2017).

21. Inchauspe, G., Nagpal, S. & Ostrove, J. M. Mapping of two varicella-zoster virus-encoded genes that activate the expression of viral early and late genes. *Virology* **173,** 700–709 (1989).

22. Strassheim, S. *et al.* Oncogenic Marek's disease herpesvirus encodes an isoform of the conserved regulatory immediate early protein ICP27 generated by alternative promoter usage. *J Gen Virol* **97,** 2399–2410 (2016).

23. Wakeman, B. S., Izumiya, Y. & Speck, S. H. Identification of Novel Kaposi's Sarcoma-Associated Herpesvirus Orf50 Transcripts: Discovery of New RTA Isoforms with Variable Transactivation Potential. *Journal of Virology* **91,** (2017).

24. Collins-McMillen, D. *et al.* Alternative promoters drive human cytomegalovirus reactivation from latency. *Proc Natl Acad Sci USA* **116,** 17492–17497 (2019).

25. Jackers, P. *et al.* Characterization of regulatory functions of the varicella-zoster virus gene 63-encoded protein. *Journal of Virology* **66,** 3899–3903 (1992).

26. Lynch, J. M., Kenyon, T. K., Grose, C., Hay, J. & Ruyechan, W. T. Physical and functional interaction between the varicella zoster virus IE63 and IE62 proteins.

Virology **302,** 71–82 (2002).

27. Bontems, S. *et al.* Phosphorylation of varicella-zoster virus IE63 protein by casein kinases influences its cellular localization and gene regulation activity. *J Biol Chem* **277,** 21050–21060 (2002).

28. Moriuchi, H., Moriuchi, M., Straus, S. E. & Cohen, J. I. Varicella-zoster virus (VZV) open reading frame 61 protein transactivates VZV gene promoters and enhances the infectivity of VZV DNA. *Journal of Virology* **67,** 4290–4295 (1993).

29. Penkert, R. R. & Kalejta, R. F. Tegument protein control of latent herpesvirus establishment and animation. *Herpesviridae* **2,** 3 (2011).

30. Kim, J. Y., Mandarino, A., Chao, M. V., Mohr, I. & Wilson, A. C. Transient Reversal of Episome Silencing Precedes VP16-Dependent Transcription during Reactivation of Latent HSV-1 in Neurons. *PLoS Pathog* **8,** e1002540 (2012).

31. Wilson, A. C. & Mohr, I. A cultured affair: HSV latency and reactivation in neurons. *TRENDS in Microbiology* **20,** 604–611 (2012).

32. Du, T., Zhou, G. & Roizman, B. HSV-1 gene expression from reactivated ganglia is disordered and concurrent with suppression of latency-associated transcript and miRNAs. *Proc Natl Acad Sci USA* **108,** 18820–18824 (2011).

33. Tegenge, M. A. *et al.* Curcumin protects axons from degeneration in the setting of local neuroinflammation. *Exp. Neurol.* **253,** 102–110 (2014).

34. Sadaoka, T. *et al.* Varicella-Zoster Virus ORF49 Functions in the Efficient Production of Progeny Virus through Its Interaction with Essential Tegument Protein ORF44. *Journal of Virology* **88,** 188–201 (2014).

35. Li, H. Minimap2: pairwise alignment for nucleotide sequences. *Bioinformatics* **34,** 3094–3100 (2018).

36. Li, H. *et al.* The Sequence Alignment/Map format and SAMtools. *Bioinformatics* **25,** 2078–2079 (2009).

37. Quinlan, A. R. BEDTools: The Swiss-Army Tool for Genome Feature Analysis. *Curr Protoc Bioinformatics* **47,** 11.12.1–34 (2014).

38. Ouwendijk, W. J. D. *et al.* T-Cell tropism of simian varicella virus during primary infection. *PLoS Pathog* **9,** e1003368 (2013).

39. Lenac Roviš, T. *et al.* Comprehensive analysis of varicella-zoster virus proteins using a new monoclonal antibody collection. *Journal of Virology* **87,** 6943–6954 (2013).

40. Okuno, T., Yamanishi, K., Shiraki, K. & Takahashi, M. Synthesis and processing of glycoproteins of Varicella-Zoster virus (VZV) as studied with monoclonal antibodies to VZV antigens. *Virology* **129,** 357–368 (1983).

41. Kennedy, P. G., Grinfeld, E., Bontems, S. & Sadzot-Delvaux, C. Varicella-Zoster virus gene expression in latently infected rat dorsal root ganglia. *Virology* **289,** 218–223 (2001).

FIGURE LEGENDS

Figure 1. Transcription profile across the VLT and ORF63 loci during lytic VZV infection of human sensory neurons and epithelial cells. **a** Coverage plots denoting dRNA-Seq (ARPE-19 epithelial cells, dark blue) and cDNA-seq (HSN, light blue) data aligned to the top strand of the VZV genome. dRNA-Seq data is representative of two independently sequenced biological replicates with RNA was extracted from lytically VZV-infected ARPE-19 cells at 4 days post-infection (4 dpi). cDNA-Seq data was generated from a pool of biological replicates collected from lytically-infected HSN at 14 dpi. Schematics of the major transcripts from VLT and ORF63 loci are shown in following colors: lytic VLT isoform (red), canonical ORF63 (light green), lytic VLT-ORF63 isoforms (purple) and latent VLT isoform (orange). **b** Analysis of VLT, ORF63 and VLT-ORF63 isoform expression by RT-qPCR analysis using the same two independent experiments in ARPE-19 cells (black) and HSN (white) for long read sequencing. Data represent mean ± SEM (standard error of mean). The primer location used for RT-qPCR analysis detecting transcripts from VLT to ORF63 loci are depicted in Supplementary Figure 1.

Figure 2. Transcription profile across the VLT and ORF63 loci in latently VZV-infected human trigeminal ganglia. **a** Detection of VLT, canonical ORF63 and VLT-ORF63 isoforms by RT-qPCR analysis in latently VZV-infected human trigeminal ganglia (TG) (n=4; post-mortem interval 4 - 4.5 hr). Data on individual TG samples are shown as unique symbols. **b** Detection of VZV ORF63 and VLT RNA by multiplex fluorescent *in situ* hybridization

(ISH) on human TG (upper two panels) and human herpes zoster skin biopsy (bottom panel). Asterisks indicate autofluorescent lipofuscin granules in neurons. Arrowheads indicate ORF63 (red) and/or VLT (green) ISH signal. Right panels: enlargements of area indicated by white box. **c** Putative transcription start sites (TSS) of VLT (row 1, blue arrows), VLT-ORF63 (row 2, green arrows) in human TGs and VLT in latently VZV-infected HSN (row 3, red arrows), as determined by 5'-RACE analysis. Schematic top shows major latent VLT and VLT-ORF63 transcript isoforms and location of primers used for 5'-RACE analysis. Bottom: VLT sequence of VLT exon 1, as previously determined by RNA-seq on human TGs[7]. Flanking regions are shown with arrows indicating putative TSS by 5'-RACE analysis.

Figure 3. Protein coding potential of VLT-ORF63 fusion transcripts. **a** Schematic presentation of VLT and VLT-ORF63 isoform transcripts with predicted encoded proteins. White boxes with solid line indicate common exons of lytic and latent isoforms of VLT and VLT-ORF63 transcripts, a box with dotted line indicates exon A of the lytic isoforms and a black box indicates a part of ORF63 5'-UTR in canonical ORF63 transcript. The end of VLT-ORF63 transcripts indicates stop codon for ORF63 CDS. Black horizontal lines indicate location of encoded open reading frames (ORFs). Blue square indicates first start codon, red triangle indicates first stop codon, green diamond indicates start codon of canonical ORF63, and grey circle indicates downstream ATG sequences. Pointed rectangles show translated protein from corresponding ORFs with a black box indicating the 24 amino acid linker peptides translated from a part of ORF63 5'-UTR in the canonical

ORF63 transcript. UTR; untranslated region, CDS; coding sequence. **b-d** Confocal microscopic images of ARPE-19 cells **b** transfected with CS-CA-VZV plasmids (48 hr post-transfection), **c** lytically infected with VZV (4 dpi), and **d** herpes zoster skin lesions. **b, c** Cells were stained with anti-pORF63 mAb (green) and anti-pORF63 pAb (red) for CS-CA-ORF63, and anti-pVLT-ORF63 pAb (green), anti-pVLT pAb (red) and anti-pORF63 mAb (blue) for CS-CA-VLT-ORF63a and CS-CA-VLT-ORF63b and lytic VZV infection. Nuclei were stained with DAPI (cyan) and images are representative of results from two independent experiments. Magnification; x600 and x3 digital zoom with 5 µm scale bars and x600 and x2 digital zoom with 10 µm scale bars. **d** Nuclei were stained with DAPI (blue) and images are representative for two independent stainings performed on one control and two herpes zoster skin biopsies. Magnification: x200 with 50 µm scale bars and x200 and x3 digital zoom with 20 µm scale bars.

Figure 4. Effect of anisomycin treatment on VZV transcription in latently VZV-infected sensory neurons in vitro. **a** RT-qPCR analysis for transcription across VLT and ORF63 loci in latently VZV-infected HSN cultures (n=3). Data on individual HSN culture experiments are shown as unique symbols. **b, c** Latently VZV-infected HSN cultures were depleted of neurotropic factors (NGF, GDNF, BDNF and NT-3) and treated with anti-NGF antibody (Ab) for 14 days. In total, n=40 independent cultures were subjected to reactivation and one representative example of a HSN culture showing complete reactivation (black circle in **c**) and early reactivation (white circle in **c**) by **b** infectious focus forming assay after transferring HSN onto ARPE-19 cells and **c** RT-qPCR analysis using HSN. **d, e** HSN cultures

were treated with **d** anisomycin (n= 3), or **e** DMSO as solvent control (n= 2) at both the somal and axonal compartment for 1 hr, washed twice and cultured for 7 days before RT-qPCR analysis. Data on individual HSN culture experiments are shown as unique symbols. Only VLT exon1-2 is shown as representative of VLT.

Figure 5. Effect of ectopic VLT-ORF63 expression on VZV gene expression in latently VZV-infected sensory neurons in vitro. At 14 days after establishment of VZV latency in HSN, following VZV genes were transduced by replication incompetent lentivirus vectors: **a** empty vector, **b** ORF63, **c** VLT-ORF63b and **d** VLT-ORF63a. Transduced cells were cultured for 14 days (n=4 replicates/vector) and subjected to RT-qPCR analysis. Technical duplicates were utilized per sample and two biologically independent data is shown.

Supplementary Figure 1. Location of primer sets detecting transcripts from VLT and ORF63 loci. Schematics of major transcripts from VLT and ORF63 loci are shown in color: lytic VLT isoform (red), latent VLT isoform (orange), canonical ORF63 (light green) and lytic VLT-ORF63 isoforms (purple). Location of primer sets used for RT-qPCR analysis to detect transcripts from VLT and ORF63 loci are depicted.

Supplementary Figure 2. Detection of VZV ORF63 and VLT RNA by fluorescent multiplex in situ hybridization. Detection of VZV ORF63 and VLT RNA by multiplex fluorescent *in situ* hybridization (mFISH) on **a** lytically VZV-infected ARPE-19 cells and **b** latently VZV-

infected human TG. **a, b** Right panels represent enlargements of area indicated by white box. **b** Rare detection of ORF63 (red) and VLT (green) as discrete puncta in nuclei of human TG neurons. Asterisks indicate autofluorescent lipofuscin granules in neurons and arrowheads indicate ORF63 and/or VLT mFISH signal. **c** Human TG were stained with mFISH using positive [UBC (red) and MALAT1 (green)] and negative control probes (DAPB, green) to demonstrate specificity of the mFISH assay and RNA integrity of the tissue assayed. Nuclei were stained with Hoechst (blue).

Supplementary Figure 3. In silico translation of VLT, canonical ORF63 and VLT-ORF63 fusion transcripts. Amino acid (aa) sequence of VLT protein (pVLT; encoded by VLT or VLT-ORF63b), ORF63 protein (pORF63; encoded by ORF63 or VLT-ORF63c), VLT-ORF63 protein (pVLT-ORF63; encoded by VLT-ORF63a) and pORF63-N+ (encoded by VLT-ORF63b). The sequence of 24 aa peptide used as immunogen to generate the chicken anti-pVLT-ORF63 polyclonal antibody is highlighted in grey color.

Supplementary Figure 4. Protein coding potential of VLT-ORF63 fusion transcripts. Immunoblotting analysis using antibodies directed to pVLT and pORF63 in the context of mock- or VZV-infection in CS-CA-empty or CS-CA-VZV transfected ARPE-19 cells. Red squares indicate pVLT-ORF63 (45.989-kDa), green triangles indicate pVLT (14.728-kDa), blue circle indicates pORF63 (30.494-kDa) and purple diamonds indicate pORF63-N+ (40.723-kDa). Images are representative of two independent experiments. Molecular weight marker (kDa) is shown in left.

Supplementary Figure 5. Transduced HSN express ectopic proteins encoded by replication incompetent lentivirus vectors. Confocal analysis using antibodies against pORF63 and pVLT in HSN transduced with replication incompetent lentivirus vectors encoding the following ORFs: **a** no gene (empty), **b** ORF63, **c** VLT-ORF63a or **d** VLT-ORF63b. HSN cultures were maturated for 49 days and transduced with each vector for 14 days. The signal obtained with anti-pORF63 mAb staining was observed in the nucleus of both ORF63- and VLT-ORF63-transduced HSN, in cytoplasm of ORF63-transduced HSN, but undetectable in HSN transduced with empty vector or VLT-ORF63b. The anti-pVLT pAb showed a nonspecific cytoplasmic signal in all transduced HSN, including 'empty', and was too strong to determine if pVLT alone is expressed by VLT-ORF63b transduction. Nuclear specific signal by anti-pVLT pAb was only detected in VLT-ORF63a-transduced HSN and co-localized with the pORF63 signal, indicating nuclear expression of pVLT-ORF63.

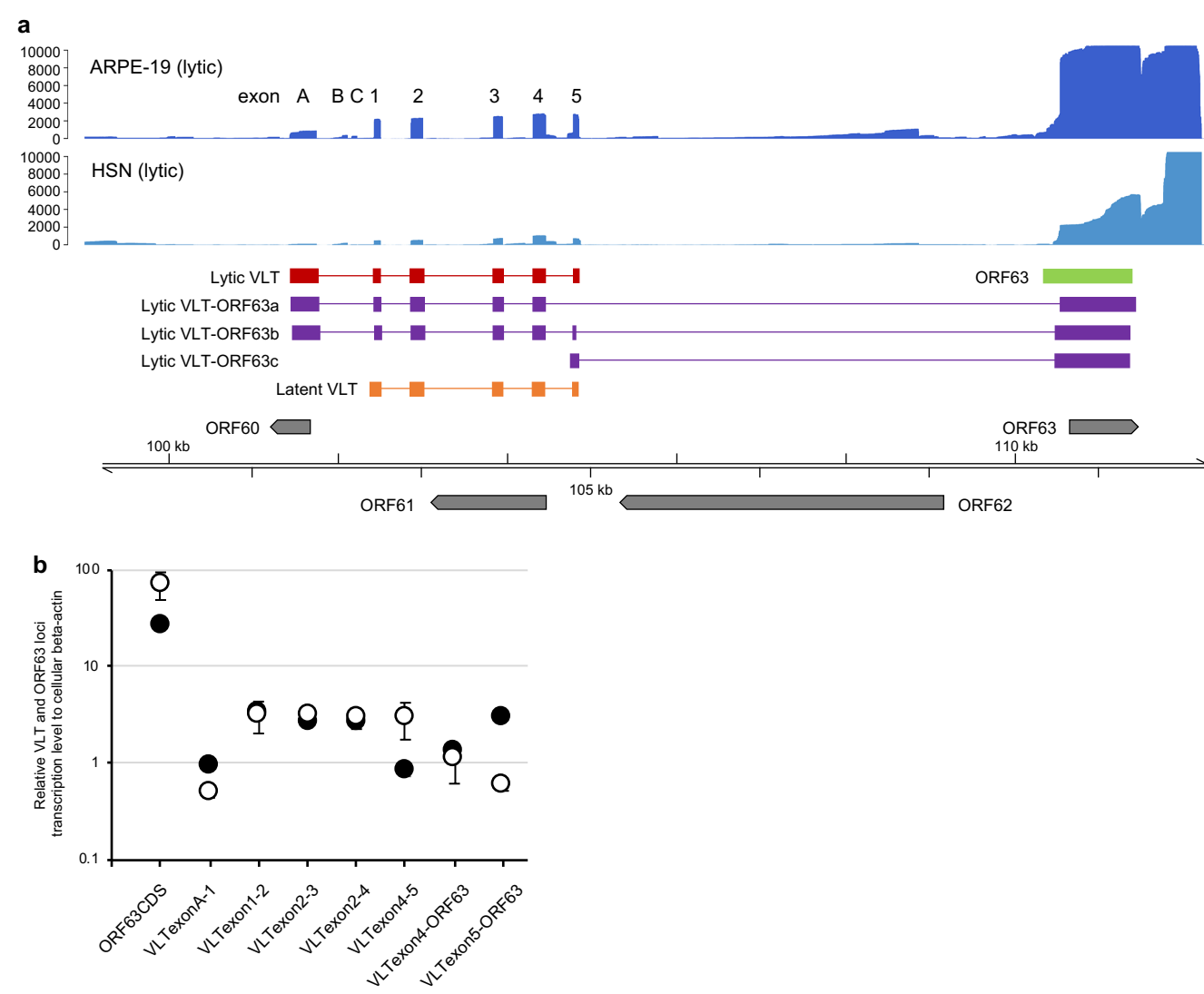

Figure 1. Transcription profile across the VLT and ORF63 loci during lytic VZV infection of human sensory neurons and epithelial cells. **a** Coverage plots denoting dRNA-Seq (ARPE-19 epithelial cells, dark blue) and cDNA-seq (HSN, light blue) data aligned to the top strand of the VZV genome. dRNA-Seq data is representative of two independently sequenced biological replicates with RNA was extracted from lytically VZV-infected ARPE-19 cells at 4 days post-infection (4 dpi). cDNA-Seq data was generated from a pool of biological replicates collected from lytically-infected HSN at 14 dpi. Schematics of the major transcripts from VLT and ORF63 loci are shown in following colors: lytic VLT isoform (red), canonical ORF63 (light green), lytic VLT-ORF63 isoforms (purple) and latent VLT isoform (orange). **b** Analysis of VLT, ORF63 and VLT-ORF63 isoform expression by RT-qPCR analysis using the same two independent experiments in ARPE-19 cells (black) and HSN (white) for long read sequencing. Data represent mean ± SEM (standard error of mean). The primer location used for RT-qPCR analysis detecting transcripts from VLT to ORF63 loci are depicted in Supplementary Figure 1.

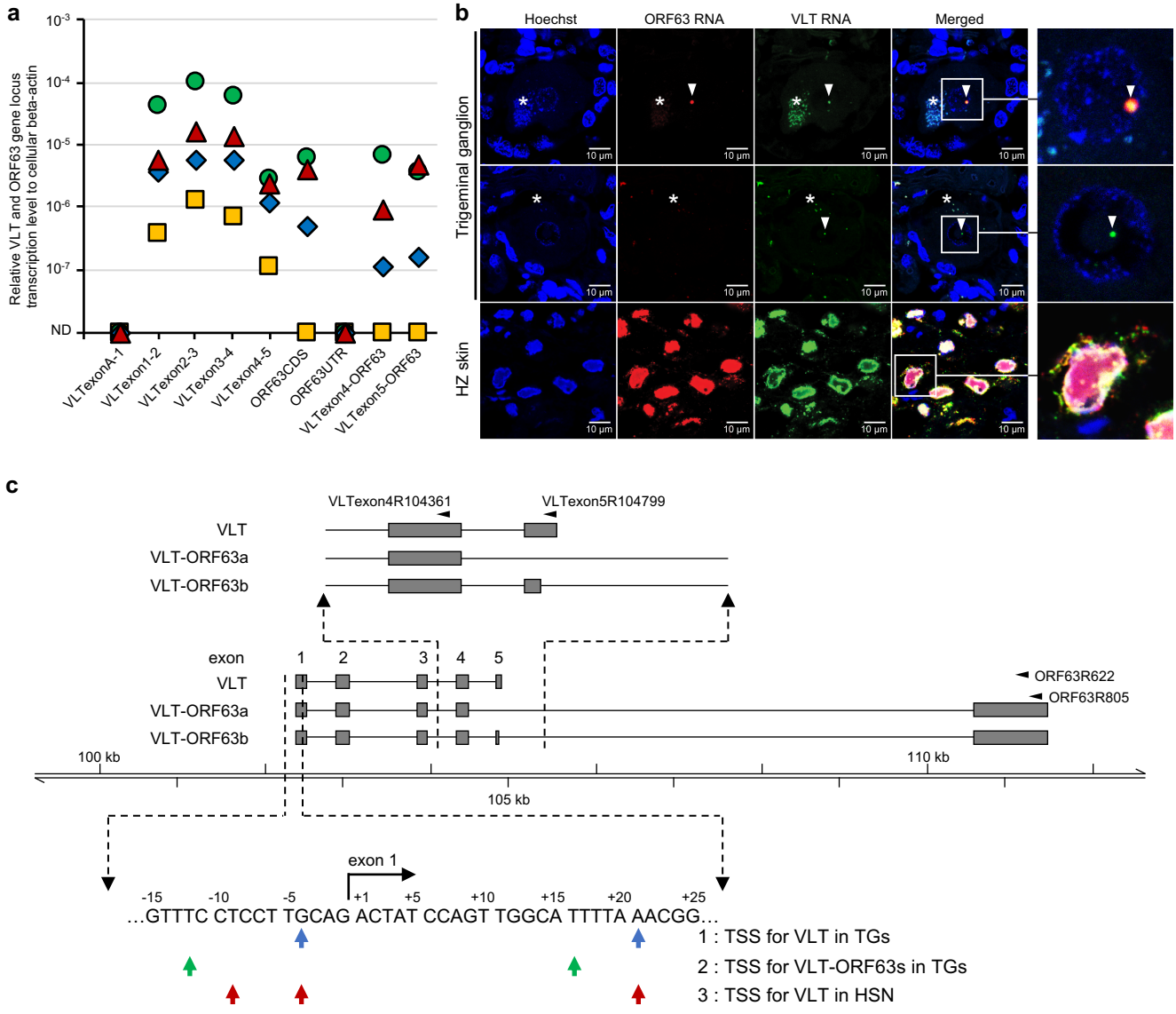

Figure 2. Transcription profile across the VLT and ORF63 loci in latently VZV-infected human trigeminal ganglia. **a** Detection of VLT, canonical ORF63 and VLT-ORF63 isoforms by RT-qPCR analysis in latently VZV-infected human trigeminal ganglia (TG) (n=4; post-mortem interval 4 - 4.5 hr). Data on individual TG samples are shown as unique symbols. **b** Detection of VZV ORF63 and VLT RNA by multiplex fluorescent *in situ* hybridization (ISH) on human TG (upper two panels) and human herpes zoster skin biopsy (bottom panel). Asterisks indicate autofluorescent lipofuscin granules in neurons. Arrowheads indicate ORF63 (red) and/or VLT (green) ISH signal. Right panels: enlargements of area indicated by white box. **c** Putative transcription start sites (TSS) of VLT (row 1, blue arrows), VLT-ORF63 (row 2, green arrows) in human TGs and VLT in latently VZV-infected HSN (row 3, red arrows), as determined by 5'-RACE analysis. Schematic top shows major latent VLT and VLT-ORF63 transcript isoforms and location of primers used for 5'-RACE analysis. Bottom: VLT sequence of VLT exon 1, as previously determined by RNA-seq on human TGs[7]. Flanking regions are shown with arrows indicating putative TSS by 5'-RACE analysis.

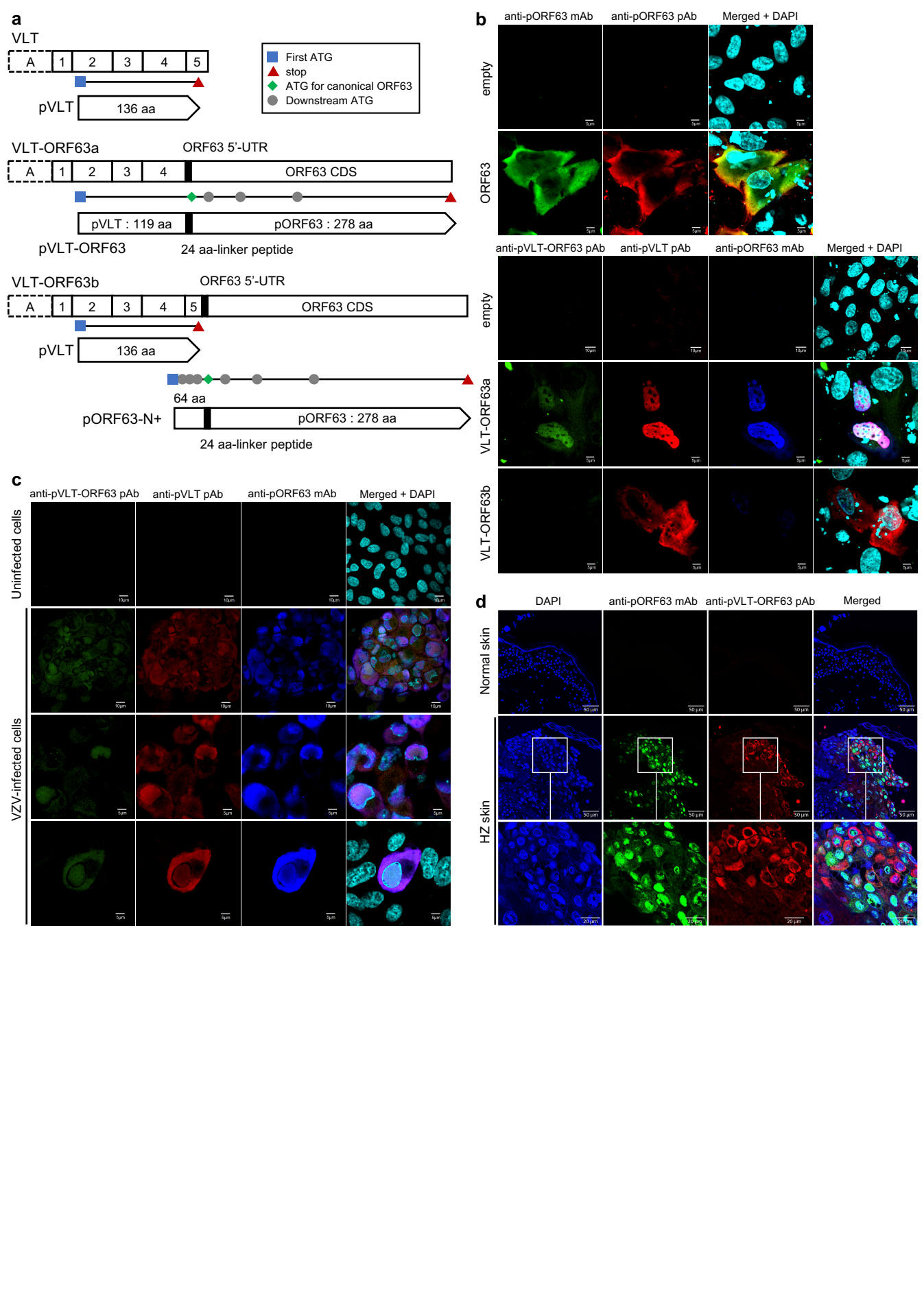
a
VLT
A
1
2
3
4
5
pVLT
136 aa
First ATG
stop
ATG for canonical ORF63
Downstream ATG
VLT-ORF63a
ORF63 5'-UTR
ORF63 CDS
pVLT : 119 aa
pORF63 : 278 aa
pVLT-ORF63
24 aa-linker peptide
VLT-ORF63b
64 aa
pORF63-N+
b
anti-pORF63 mAb
anti-pORF63 pAb
Merged + DAPI
empty
ORF63
anti-pVLT-ORF63 pAb
anti-pVLT pAb
VLT-ORF63a
VLT-ORF63b
c
Uninfected cells
VZV-infected cells
d
DAPI
Normal skin
HZ skin

Figure 3. Protein coding potential of VLT-ORF63 fusion transcripts. **a** Schematic presentation of VLT and VLT-ORF63 isoform transcripts with predicted encoded proteins. White boxes with solid line indicate common exons of lytic and latent isoforms of VLT and VLT-ORF63 transcripts, a box with dotted line indicates exon A of the lytic isoforms and a black box indicates a part of ORF63 5'-UTR in canonical ORF63 transcript. The end of VLT-ORF63 transcripts indicates stop codon for ORF63 CDS. Black horizontal lines indicate location of encoded open reading frames (ORFs). Blue square indicates first start codon, red triangle indicates first stop codon, green diamond indicates start codon of canonical ORF63, and grey circle indicates downstream ATG sequences. Pointed rectangles show translated protein from corresponding ORFs with a black box indicating the 24 amino acid linker peptides translated from a part of ORF63 5'-UTR in the canonical ORF63 transcript. UTR; untranslated region, CDS; coding sequence. **b-d** Confocal microscopic images of ARPE-19 cells **b** transfected with CS-CA-VZV plasmids (48 hr post-transfection), **c** lytically infected with VZV (4 dpi), and **d** herpes zoster skin lesions. **b, c** Cells were stained with anti-pORF63 mAb (green) and anti-pORF63 pAb (red) for CS-CA-ORF63, and anti-pVLT-ORF63 pAb (green), anti-pVLT pAb (red) and anti-pORF63 mAb (blue) for CS-CA-VLT-ORF63a and CS-CA-VLT-ORF63b and lytic VZV infection. Nuclei were stained with DAPI (cyan) and images are representative of results from two independent experiments. Magnification; x600 and x3 digital zoom with 5 µm scale bars and x600 and x2 digital zoom with 10 µm scale bars. **d** Nuclei were stained with DAPI (blue) and images are representative for two independent stainings performed on one control and two herpes zoster skin biopsies. Magnification: x200 with 50 µm scale bars and x200 and x3 digital zoom with 20 µm scale bars.

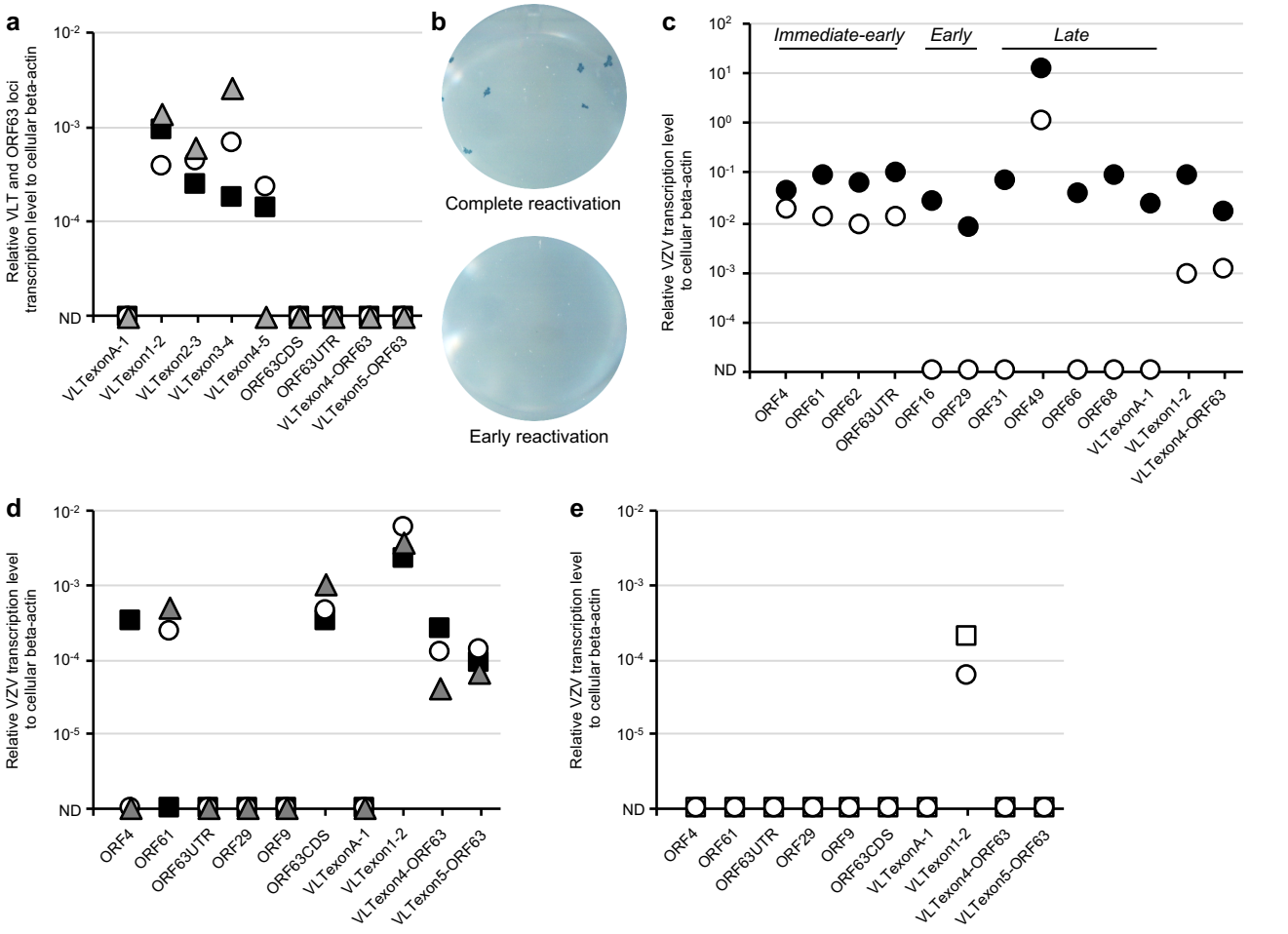

Figure 4. Effect of anisomycin treatment on VZV transcription in latently VZV-infected sensory neurons in vitro. **a** RT-qPCR analysis for transcription across VLT and ORF63 loci in latently VZV-infected HSN cultures (n=3). Data on individual HSN culture experiments are shown as unique symbols. **b, c** Latently VZV-infected HSN cultures were depleted of neurotropic factors (NGF, GDNF, BDNF and NT-3) and treated with anti-NGF antibody (Ab) for 14 days. In total, n=40 independent cultures were subjected to reactivation and one representative example of a HSN culture showing complete reactivation (black circle in **c**) and early reactivation (white circle in **c**) by **b** infectious focus forming assay after transferring HSN onto ARPE-19 cells and **c** RT-qPCR analysis using HSN. **d, e** HSN cultures were treated with **d** anisomycin (n= 3), or **e** DMSO as solvent control (n= 2) at both the somal and axonal compartment for 1 hr, washed twice and cultured for 7 days before RT-qPCR analysis. Data on individual HSN culture experiments are shown as unique symbols. Only VLT exon1-2 is shown as representative of VLT.

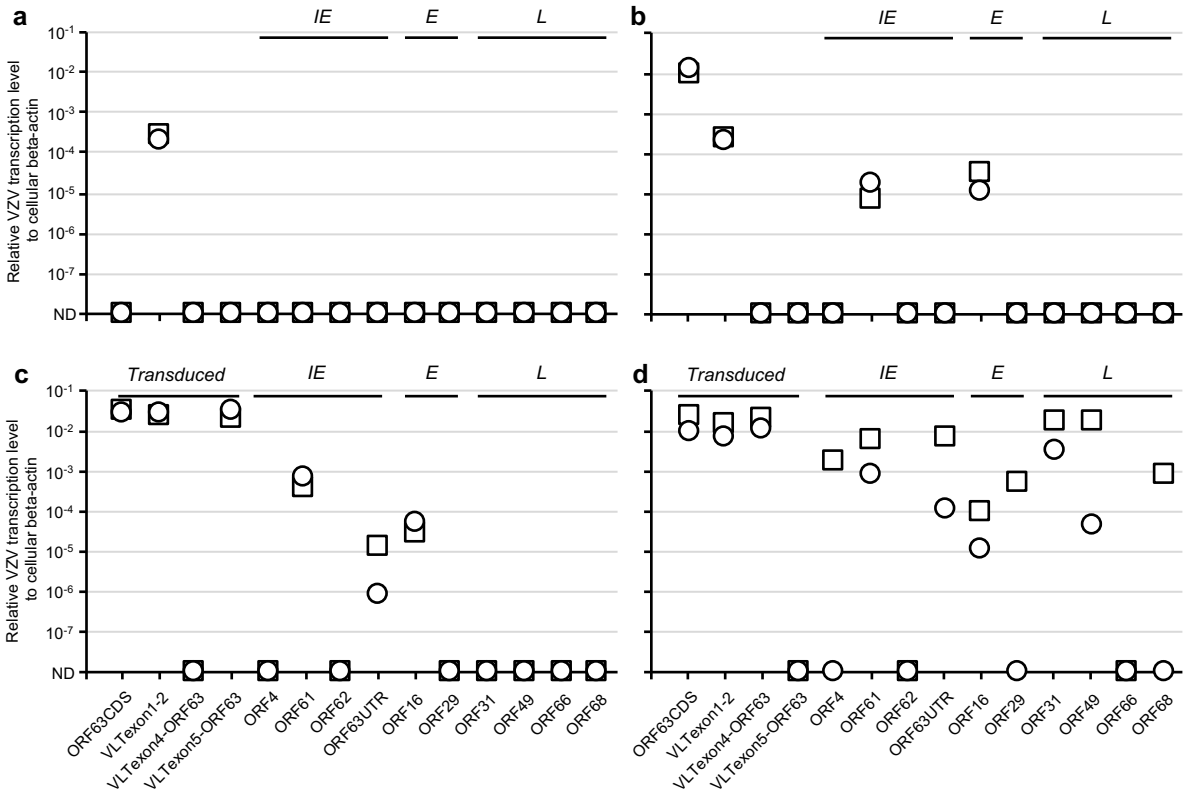

Figure 5. Effect of ectopic VLT-ORF63 expression on VZV gene expression in latently VZV-infected sensory neurons in vitro. At 14 days after establishment of VZV latency in HSN, following VZV genes were transduced by replication incompetent lentivirus vectors: **a** empty vector, **b** ORF63, **c** VLT-ORF63b and **d** VLT-ORF63a. Transduced cells were cultured for 14 days (n=4 replicates/vector) and subjected to RT-qPCR analysis. Technical duplicates were utilized per sample and two biologically independent data is shown.